Solid State Communications 253 (2017) 14–18

Contents lists available at ScienceDirect

Solid State Communications

journal homepage: www.elsevier.com/locate/ssc

Communication

Disorder-driven electron delocalization in strange metals: The case of tetragonal FeTe

Luis Craco

Instituto de Física, Universidade Federal de Mato Grosso, 78060-900 Cuiabá, MT, Brazil

A B S T R A C T

We investigate the dual roles of electron–electron interactions and site-diagonal disorder in a strange bad-metal. Saturating- and insulating-like resistivity observed in the non-magnetically ordered phase of tetragonal FeTe are shown to be driven by the interplay between multiband effects and iron-*d* shell band-filling. Incorporation of site-diagonal disorder promotes weak electronic delocalization and metallicity in tetragonal FeTe. The correlated electronic structure we derive is promising in the sense that it leads to results that might explain why moderate disorder can generate nearly linear resistivity dependence in strange metals.

1. Introduction

In normal metals electrical resistivity $[\rho(T)]$ increases with temperature because electrons are scattered by lattice vibrations. Without intrinsic blocking by phonons, the value of $\rho(T)$ also increases with disorder because electrons are usually scattered by imperfections and impurities in the solid. However, in strongly correlated metals large metallic resistivity is mostly driven by strong inelastic scattering rates [1] and in this regime disorder effectively weakens Coulomb repulsion effects (Anderson–Mott duality), moving the system away from the Mott–Hubbard insulating state [2].

It is now recognized that the appearance of strange metal [3] and pseudogap phases [4] in correlated electron systems reveals a breakdown of the assumptions underlying Landau–Fermi liquid theory. If the Fermi-liquid (FL) quasiparticle gives away to qualitatively new electronic states in exotic metals, one expects changes in the character of low-energy excitations, manifesting itself in emergence of qualitatively new electronic behavior. In particular, these changes should manifest themselves in one- and two-particle responses [5], which probe the excitation spectrum of the system. A fundamental question here is: How can metallicity be partially restored in systems in close proximity to Mottness? In this work we answer this question, providing a description of anomalous transport seen in the tetragonal phase of FeTe. We reveal a surprising contrast between incoherent non-FL phenomena induced by multi-orbital (MO) electron–electron interaction and disorder effects.

Iron-based superconductors are among the latest examples of materials showing unconventional normal state properties [6,7]. In $SmFeAsO_{1-x}F_x$ [8], for example, suppression of superconductivity by high magnetic fields reveals a low-T insulator-like state, as in underdoped cuprates [9]. Of particular importance here are the 11-iron chalcogenides, which have been synthesized with various compositions and conditions [10–13], showing different degrees of electronic correlations and disorder effects in their normal state properties [14–17]. While crystallographically simpler than the pnictides and oxyarsenides systems, the 11-family exhibits a host of anomalous physical responses, including strange metallic and insulating-like [12,13,18–20] normal state resistivity above the superconducting transition temperature, T_C. Particularly, tetragonal FeSe exhibits superconductivity with $T_C = 9$ K [21]. which can be enhanced up to 100 K if the sample is grown on $SrTiO_3(001)$ [22]. FeSe is sensitive to stoichiometry – minute non-stoichiometry in $Fe_{1+y}Se_{1-x}$ seems to destroy the superconducting state [23]. On the other hand, the non-superconducting $Fe_{1+y}Te$ exhibits a first-order structural phase transition and simultaneously develops long-range antiferromagnetic order below 65 K [24].

Extant experimental studies of transition-metal (M) or chalcogen (Se,Te) ion substitution and Fe-excess on magnetic, superconducting and normal state properties of $Fe_{1+y-z}M_zSe_{1-x}Te_x$ systems show disorder [11,15–17] and electron correlation fingerprints [14,25]. In non-superconducting $Fe_{1+y}Te$, the effect of Fe-excess (y) is to reduce the electrical resistivity and the Néel temperature [13]. Interestingly, similar effect is also seen in $Fe_{1+y}Se_{1-x}Te_x$ solid solutions [12,26], suggesting disorder induced many-body delocalization in these systems. This behavior is consistent with other experimental studies on $Fe_{1+y}Te_{1-x}Se_x$ systems, indicating that reducing y antiferromagnetism is suppressed and superconductivity is favored [11,16]. We shall notice here the work by Sun et al. [27] showing that Se substitution of Te in

E-mail address: lcraco@fisica.ufmt.br.

http://dx.doi.org/10.1016/j.ssc.2017.01.024
Received 24 November 2016; Received in revised form 17 January 2017; Accepted 24 January 2017
Available online 27 January 2017

$Fe_{1+y}Te_{1-x}Se_x$ has similar effect. The underlying effect that results from transition-metal [28] or chalcogen substitution [27] is to suppress the structural transition and magnetic order via an yet ill understood mechanism of chemical modification in unconventional metals. Needless to say, a proper microscopic description of localization–delocalization transition in 11 iron-chalcogenide systems is important for understanding the role played by dynamical correlations in the low-energy electronic states of iron-based superconductors in general. In this work we provide new insights to the fascinating problem of concomitant alloy disorder and Coulomb correlation effects in pure and electron-doped FeTe, revealing a dual response to these perturbations.

A microscopic treatment of combined site-diagonal disorder and multiband electronic correlations in FeTe is important for understanding the evolution from an orbital-blocked phase [29] to a distinct incoherent electronic state and its implications to superconductivity [30,31]. Most of the currently theoretical understanding of $Fe_{1+y-z}M_zTe_{1-x}Se_x$ alloys is restricted to one-electron band structure calculations [32–35]. Specifically, local-density-approximation plus coherent-potential-approximation (LDA+CPA) study by Sing [32] shows that the Fe d-bands are somewhat broadened by disorder due to chalcogen modification, resulting in smeared Fermi surfaces. Physically, the reason for this finding is that the Se(Te) bands lie far from E_F, whereby disorder scattering does influence the chalcogen bands, but has a smaller effect on the Fe $3d$ states (limited to a broadening of the d-bands). Thus, as found by Singh, including disorder via chemical modification will still give a metallic state as a function of x in $FeSe_{1-x}Te_x$, and so static disorder by itself cannot rationalize the observation of strong normal state incoherence as well as the finite T crossover to insulator-like behavior as a function of x in Fe(Se,Te) solid solutions [13,20,36,37], and the same holds true for transition-metal substitution in $Fe_{1+y-z}M_zTe_{1-x}Se_x$ alloys [33,34]. On the other hand, as shown for FeTe [29,38] and FeSe [39,40] a correlation based approach is needed to describe exotic [41] features observed in experiment. With this caveats in mind, we undertake here a LDA+dynamical-mean-field-theory (LDA+DMFT) study of site-diagonal disorder in FeTe, showing how weak electronic delocalization seen in transport [12,13,16,17,19] can be understood within a single theoretical picture. Good semiquantitative agreement with resistivity data of $Fe_{1.05}Te$ [42] serves as support to our proposal of coexisting dynamical correlation and disorder effects in Fe-chalcogenide solid solutions.

2. LDA+DMFT: theory and discussion

The relevant inputs to our theory are the LDA DOS for the five $3d$ orbitals already discussed in Ref. [38], the local Coulomb interactions and Hund's coupling, J_H. With this the correlated many-body Hamiltonian for FeTe in the absence of alloy disorder reads

$$H = \sum_{\mathbf{k},a,\sigma} \epsilon_{\mathbf{k},a} c^{\dagger}_{\mathbf{k},a,\sigma} c_{\mathbf{k},a,\sigma} + U \sum_{i,a} n_{ia\uparrow} n_{ia\downarrow} + U' \sum_{i,a\neq b} n_{ia} n_{ib} - J_H \sum_{i,a\neq b} \mathbf{S}_{ia} \cdot \mathbf{S}_{ib}. \quad (1)$$

Here, $a = (x^2 - y^2, 3z^2 - r^2, xz, yz, xy)$ denote the diagonalized $3d$ orbitals of FeTe, $\epsilon_a(\mathbf{k})$ is the one-electron band dispersion, which encodes details of the band structure, and U, $U'(=U - 2J_H)$ are the intra- and inter-orbital Coulomb terms. We evaluate the many-particle Green's functions of the Hamiltonian above within LDA+DMFT [43], using MO iterated perturbation theory (MO-IPT) as impurity solver [44,45]. The DMFT solution involves replacing the lattice model by a self-consistently embedded MO-Anderson impurity model, and the self-consistency condition requiring the local impurity Green's function to be equal to the local Green's function for the lattice. The full set of equations for the MO case can be found, for example, in Ref. [44].

An advantage of the LDA+DMFT approximation is that all electronic properties are rigorously understood solely in terms of local one-particle spectral functions [47]. In an earlier work [38], it was shown that the unconventional transport properties of electron doped FeTe can be understood using LDA+DMFT with sizable d band correlations. Here, we extend this to characterize the pseudogap phase of disordered tetragonal FeTe in depth. Specifically, we compute the temperature dependence of the dc resistivity $[\rho_{dc}(T)]$, and correlate with the evolution of the DMFT spectral functions, $A_a(\mathbf{k}, \omega)$. Within the Kubo formalism [48], the dc-conductivity can be expressed as [49]

$$\sigma_{dc}(T) = \pi e^2 v^2 \sum_a \int d\epsilon \rho_a^{(0)}(\epsilon) \int d\omega A_a^2(\epsilon, \omega)[-f'(\omega)],$$

where $\rho_a^{(0)}(\epsilon)$ is the LDA DOS of the five $3d$-bands, v is the electron's velocity and $f(\omega)$ is the Fermi function. For the sake of simplicity the approximation made here is to ignore the $\mathbf{k}$-dependence of electron's velocity, $v_{\mathbf{k},a}$. In this situation, following Saso et al. [50] we approximate $v_{\mathbf{k},a}$ by a single average carrier velocity (v) for all orbitals. In fact, it has been shown [50,51] that this assumption works well for numerical computations of optical conductivity responses for correlated multi-band systems, including iron-based superconducting materials, supporting our approximation in $\sigma_{dc}(T)$ above. In our theory, the observed features in resistivity $\rho_{dc}(T) \equiv 1/\sigma_{dc}(T)$ originate from filling-controlled or disorder-induced spectral changes.

In order to address the role of alloy disorder in the non-magnetically ordered state of pure and electron-doped FeTe, below we present LDA+DMFT results for fixed values of U=4 eV and $J_H = 0.7$ eV. Here we follow Ref. [29], which also employed fixed Coulomb interaction parameters to study a series of Fe-based materials, confirming that changes in their physical properties are mainly due to variations in the one-band structural inputs and small differences in the total electron occupation (n) of the iron $3d$-shell, rather than changes in the screening of the MO Coulomb interactions [52] or by the mutual interplay between U, U' and J_H [53].

To begin with, we show in Fig. 1 the effect of electron-doping on the dc resistivity of FeTe in the absence of disorder. One striking feature of our results for pure $(n = 6.0)$ and electron-doped $(n = 6.4)$ FeTe is the saturating resistivity at room temperature. Similar trend has been observed in the parent and transition-metal doped $SrFe_2As_2$ compound, albeit at higher temperatures [54], which is consistent with the

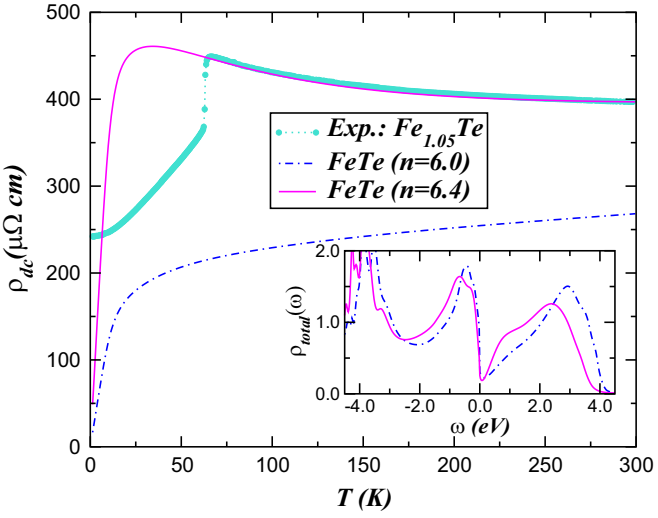

Fig. 1. (Color online) Theory-experiment comparison of resistivity versus temperature (normalized to the experimental value at 300 K) for $Fe_{1.05}Te$ [42], showing good semiquantitative agreement with experiment in the paramagnetic, non-Fermi liquid state: our results for $\rho_{dc}(T)$ are to be trusted only above the Néel temperature, T_N=65 K. As discussed in Ref. [38], observed features above 66 K are well reproduced using the spectral functions of electron-doped $(n = 6.4)$ FeTe. $[\rho_{dc}(T)$ for undoped $(n = 6.0)$ FeTe is shown for comparison.] Inset shows the total LDA+DMFT density-of-states (DOS) for the Fe $3d$ orbitals of tetragonal FeTe, for U=4 eV and J_H=0.7 eV. Large-scale transfer of spectral weight is visible upon doping.

fact that scattering caused by MO electronic correlations are stronger in 11 iron-chalcogenides compared to 122 iron-pnictides. Focusing on the electron-doped regime, we make contact with experiment by Chen et al. [42]. Similar experimental results were also obtained by other groups, [13,25,55] suggesting a common underlying low-energy scenario for FeTe. As visible in Fig. 1, our LDA+DMFT results provide a compelling description of observed experimental data [42], supporting the view of strong electronic correlations in 11 iron-chalcogenides [56]. Noteworthy, in an earlier work [38] we have clarified microscopically the origin of the insulating-like form (above $T \approx 65$ K) in FeTe. It was shown there that orbital-selective incoherence characterizes the paramagnetic phase in layered Fe(Se,Te) systems in general. According to our results the emergence of an insulating-like paramagnetic state in FeTe should be considered as a manifestation of slightly increasing the band filling via electron doping [29,57] an orbital-selective metal in close proximity to Mott localization [58]. As seen in Fig. 1, stoichiometric FeTe (n=6.0) has lower resistivity values, implying that orbital-selective localization is induced with increasing the carrier concentration of the iron d-shell. Moreover, in the inset of Fig. 1 we also display the LDA+DMFT total DOS of FeTe in the absence of disorder, showing doping induced spectral weight transfer (SWT) over large energy scales and enhancement of the lower-Hubbard (LHB) band in the electron doped case. This implies an intrinsic electronic tendency towards local moment formation [40] in the electron doped system. In addition to large-scale SWT, our results reveal that the FL-like pinning of the LDA +DMFT DOS to its LDA [38] value is completely lost for U=4 eV. Instead, the saturating [59] metallic state in FeTe shows a pseudogap-like feature close to the Fermi energy, E_F, with no evidence of (orbital-selective) FL quasiparticles. Interestingly, this effect is more pronounced in electron-doped FeTe, reflecting its close proximity to a paramagnetic Mott insulating state.

2.1. Effect of site-diagonal disorder in the tetragonal phase of FeTe

Let us now discuss the effect of site-diagonal, alloy disorder in this strange metal system. Here, we treat the MO problem of FeTe within the LDA+DMFT(MO-IPT+CPA) approach, which allows for an exact treatment of binary alloy disorder in the limit of high lattice-dimensions [60]. This treatment has been already used to describe electronic transitions of doped Mott insulators [61], which were found to be in good accordance with experimental observations. Generally speaking, our scheme is an extension of that applied to the one-band disordered Hubbard model [60], where the effect of site-diagonal disorder is modeled by adding

$$H_d = \sum_{i,a,\sigma} v_i n_{i,a,\sigma} \tag{2}$$

to Eq. (1). In the spirit of Refs. [60,62,63] we restrict ourselves to a binary-alloy distribution for disorder, therefore the disorder potentials v_i are specified by the probability distribution $P(v_i) = (1-x)\delta(v_i) + x\delta(v_i - V)$, meaning that upon incorporation of (chemical) disorder a fraction x of sites have an additional local potential V for an electron hopping onto that site. In other words, the Fe-3d carriers experience different local environments in the course of their hopping, and the physical object which accounts for this effect is the disorder-averaged local Green's function $\langle G_a(\omega)\rangle_{ii}$, with $\langle..\rangle_{ii}$ denoting the disorder average. After configurational averaging using T-matrix (CPA) approximation, all interesting dynamical effects are contained in the CPA self-energy, related to the single-site propagator [64]

$$\langle G_a(\omega)\rangle_{ii} = \frac{1-x}{\omega - \mathcal{A}_a(\omega)} + \frac{x}{\omega - V - \mathcal{A}_a(\omega)}. \tag{3}$$

Here, the dynamical Weiss function $\mathcal{A}_a(\omega)$ describes the motion of a-band electrons in the effective medium related to disorder. The combined $U+V$ (Mott–Anderson) problem, i.e., the situation where

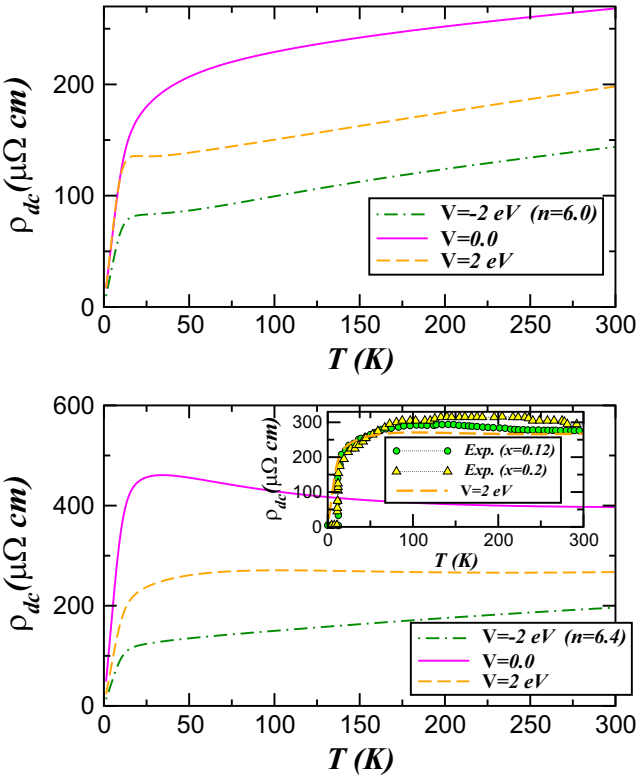

Fig. 2. (Color online) Effect of site-diagonal disorder for $x = 0.2$ in pure (upper panel) and electron-doped (lower panel) FeTe, showing reduced resistivity profiles compared to the disorder free non-Fermi liquid system. Noteworthy is the linear-T dependence of $\rho_{dc}(T)$ above 30 K for the two curves with $n = 6.0$ as well as for $V = -2.0$ eV in the electron-doped regime. Also interesting is the saturating (constant) behavior of $\rho_{dc}(T)$ for $n = 6.4$ with $V = 2.0$ eV. In the inset of the lower panel we display our theory–experiment comparison with data of annealed $Fe_{1+y}Te_{1-x}Se_x$ samples taken from Ref. [27]: notice the good agreement between experimental data and the LDA+DMFT result for $V = 2.0$ eV and $n = 6.4$.

MO Coulomb repulsion and disorder-induced electronic localization simultaneously affect the one-particle response, is treated within LDA +DMFT by a proper combination of the interaction self-energy with the CPA one. The detailed formulation of the $U+V$ problem has already been developed and used in the context of LDA+DMFT for real materials [61], so we do not repeat the equations here.

Fig. 2 summarizes our main results, showing how the T-dependence of electrical resistivity in FeTe is reshaped via alloy disorder effects. We have chosen $x = 0.2$ in $P(v_i)$ and two values for the disorder potential V in this work. A $V = -2$ eV is expected to simulate disorder effects of an almost fully occupied electron-shell [32,34], which can be induced for example by Co or Ni substitution on the Fe sub-lattice [17]. On the other hand, the opposite regime ($V = 2$ eV) accounts for site-diagonal disorder caused by empty-shell ion substitution in the iron sub-lattice. As seen, the salient features are almost the same for all variants, showing reduced resistivity values compared to the two disorder-free cases. Our results in Fig. 2 confirm that the magnitude of $\rho_{dc}(T)$ decreases with disorder in materials close to Mott transition. This is consistent with previous theoretical studies arguing that disorder effectively weakens correlation effects and moves the system away from Mottness [1,2]: the underlying physical reason is that a local random potential broadens the bare one-particle bandwidth (W), increasing the critical interaction for the Mott–Hubbard metal–insulator transition. Moreover, below a characteristic temperature, $T \approx 20$ K, we observe a downward curvature in $\rho_{dc}(T)$ down to low T. For temperatures higher than this value the evolution with temperature is smooth, indicating a low-T crossover as opposed to a first-order transition. It is worth noting, however, that the resistivity curves of

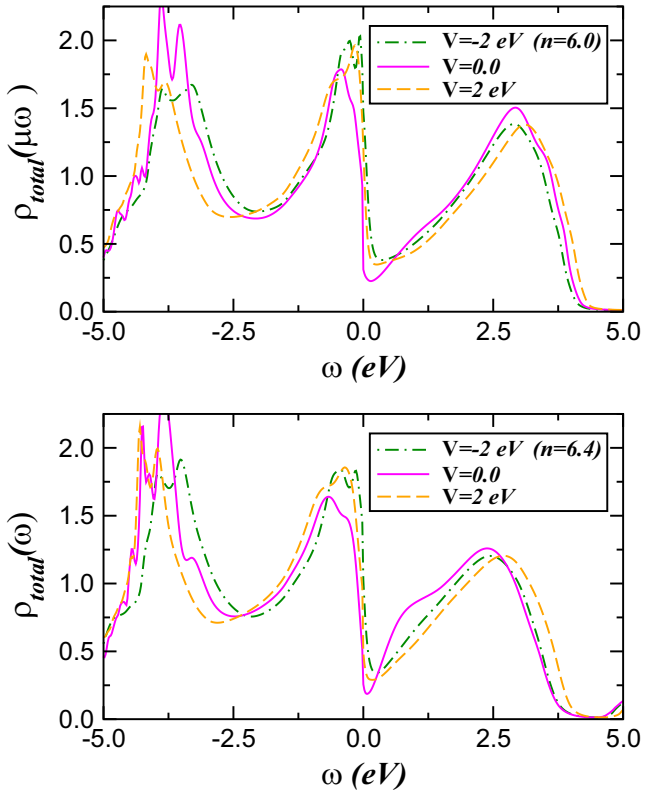

Fig. 3. (Color online) Effect of site-diagonal disorder ($x = 0.2$ for the probability distribution) in the total LDA+DMFT density-of-states (with $U = 4.0$ eV, $U' = 2.6$ eV and $J_H = 0.7$ eV) of Fe d-orbitals in stoichiometric $n = 6.0$ (top panel) and electron-doped $n = 6.4$ (lower panel) FeTe. The important difference to be seen is the appearance of low-energy electronic states near the Fermi level ($E_F = \omega = 0$) in disordered FeTe. Large-scale transfer of spectral weight induced by alloy disorder is also visible in our results. Notice the enhancement in intensity of the low-energy bump close to E_F in the valence band states of disordered FeTe.

disordered FeTe in the top panel of Fig. 2 show nearly linear T-dependence above $T \approx 33$ K, similar to hole-doped cuprate oxides [9] as well as to pressurized $SmFeAsO_{1-x}F_x$ (x=0.19) [65]. Also very suggestive is our result for electron-doped FeTe in the lower panel of Fig. 2, displaying that the resistivity for $V = 2.0$ eV flattens out and maintains an almost constant (saturating) value between 100 and 300 K. Interestingly, this behavior is in good agreement with experimental observations by Sun et al. for annealed $Fe_{1+y}Te_{1-x}Se_x$ samples. In fact, the theory–experiment agreement in the inset of Fig. 2 is a compelling evidence of MO electronic delocalization and site-diagonal disorder effects induced via chalcogen substitution in the tetragonal FeTe parent compound.

We shall end this discussion by making contact with other experiments showing similar behavior as in Fig. 2. The nearly linear T-dependence as obtained for $V = -2$ eV and $n = 6.4$ has been reported $FeSe_{0.5}Te_{0.5}$, showing similar slope and downward curvature in $\rho_{dc}(T)$ [19,66]. Our theoretical results are also consistent with an additional experimental study showing reduced resistivities in $Fe_xSe_{0.5}Te_{0.5}$ due to iron vacancies, $x < 1$ [26]. Although the presence of Fe vacancies effectively changes the charge carrier population [26], our results should be taken as a theoretical evidence that chemical disorder might be the primary origin of reduced resistivity in Fe-deficient films compared to that of a defect-free sample. However, whether disorder induced by vacancies has direct implications on T_C [67] in MO iron-superconducting materials is out of scope of this work.

Finally, we provide a possible explanation of the exotic resistivity responses discussed above in view of understanding the role of alloy disorder in incoherent non-FL metals. In Fig. 3 we show the changes on correlated electronic structure in pure (top panel) and electron-doped (bottom panel) FeTe. The most salient feature to be seen is that weak electronic delocalization occurs upon incorporation of disorder. This is characterized by the appearance of low-energy electronic states near E_F. What is the origin of these low-energy features? In a MO system like 11-iron chalcogenides, strong (incoherent) scattering between different carriers in orbital states split relative to each other due to the specific crystal field leads to two main effects: (i) It leads, via static-Hartree contributions (from the static part of the orbital-dependent self-energies) to orbital-dependent shifts of the d-bands relative to each other, and renormalized scattering rates [1] due to sizable V cause appreciable SWT over large energy scales, from high to low-energy. This second feature leads to a modification of the spectral lineshape, as shown in Fig. 3. In accordance with earlier studies [1,2,60], broadening-induced quantitative changes of the effective U/W ratio in the present case relative to disorder-free FeTe lead to less pronounced pseudogap lineshape, where enhanced low-energy spectral features within the valence band states clearly show up near E_F. Microscopically, incoherent scattering arising from co-existence of alloy-disordered and (orbital-selective) Mott-localized electronic states yields the emergence of a reconstructed via disorder pseudogaped spectral functions, similar to what is seen in angle-resolved photoemission spectroscopy (ARPES) of $FeTe_{1-x}Se_x$ ($0 \le x \le 0.45$) [31]. Noteworthy, in disordered FeTe infrared FL behavior (narrow Kondo quasiparticle resonance in DMFT) is completely extinguished by strong scattering rate associated with the breakdown of FL theory in its most basic form due to sizable U, U' and V. Thus, our incoherent metal might be a MO counterpart of the *strange* metal [3].

3. Conclusion

To summarize, we have used LDA+DMFT for a five-band Hubbard model to perform a realistic many-particle study of disorder effects in an incoherent non-Fermi-liquid metal. In particular, considering FeTe as a suitable template, we have analyzed its paramagnetic saturating metal regime, baring it as an effect of multi-orbital Hubbard interactions. An interesting behavior is obtained when we consider site-diagonal alloy disorder on this state: upon the latter, weak many-body delocalization due to reconstructed spectral functions and transfer of spectral weight from high- to low-energies prevents strong incoherent motion of electrons (induced by Mottness) intrinsic to FeTe. Our theory provides possible routes to an explanation of linear resistivity in strongly correlated non-Fermi-liquid metals. As shown here, a T-linear transport arises from dual charge-carrier scatterings due to interplay between disorder and electron correlations. This exotic behavior can be directly tested by a combination of spectral and transport measurements. Such studies are called for to corroborate our prediction for multiband materials near the Mott transition. Moreover, the interplay between disorder induced weak electronic delocalization and bad-itinerancy in FeTe suggests a promising and practical route to access electron pairing on bands without Fermi surfaces as suggested for $LiFe_{1-x}Co_xAs$ [68], but this remains to be seen in future.

Acknowledgments

This work is supported by CNPq (Grant No. 307487/2014-8). The author also thanks M.A. Gusmão for discussions as well as the Physical Chemistry Department at Technical University Dresden for hospitality.

References

[1] M.M. Radonjić, et al., Phys. Rev. B 81 (2010) 075118.
[2] K. Byczuk, et al., Phys. Rev. Lett. 94 (2005) 056404
M.A. Gusmão, Phys. Rev. B 77 (2008) 245116
R.D.B. Carvalho, M.A. Gusmão, Phys. Rev. B 87 (2013) 085122.
[3] P.W. Anderson, P.A. Casey, Phys. Rev. B 80 (2009) 094508.
[4] I. Pallecchi, et al., J. Supercond. Nov. Magn. 24 (2011) 1751.
[5] M. Klein, et al., Phys. Rev. Lett. 101 (2009) 266404

N. Doiron-Leyraud, et al., Nature 425 (2003) 595.
[6] D.C. Johnston, Adv. Phys. 59 (2010) 803
G.R. Stewart, Rev. Mod. Phys. 83 (2011) 158
K. Deguchi, et al., Sci. Technol. Adv. Mater. 13 (2012) 054303.
[7] For recent overviews on iron based superconductors see also, M.K. Wu et al., J. Phys. D: Appl. Phys. 48 (2015) 323001; Q. Si et al., Nat. Rev. Mater. 1 (2016) 16017.
[8] S.C. Riggs, et al., Phys. Rev. B 79 (2009) 212510.
[9] R.W. Hill, et al., Nature (Lond.) 414 (2001) 711
Y. Ando, et al., Phys. Rev. Lett. 93 (2004) 267001.
[10] J. Wen, et al., Rep. Prog. Phys. 74 (2011) 124503
Z. Xu, et al., Phys. Rev. B 89 (2014) 174517.
[11] R. Viennois, et al., J. Solid State Chem. 183 (2010) 769.
[12] M. Onoda, et al., J. Phys.: Condens. Matter 22 (2010) 505702.
[13] T.J. Liu, et al., Phys. Rev. B 80 (2009) 174509.
[14] A. Pourret, et al., Phys. Rev. B 83 (2011) 020504 (R)
J. Hu, et al., Phys. Rev. B 83 (2011) 134521.
[15] N.L. Saini, Sci. Technol. Adv. Mater. 14 (2013) 014401.
[16] T. Gebre, G. Li, J.B. Whalen, B.S. Conner, et al., Phys. Rev. B 84 (2011) 174517.
[17] C. Koz, et al., Phys. Rev. B 93 (2016) 024504.
[18] P.-H. Lin, et al., Phys. Rev. Lett. 111 (2013) 217002.
[19] D. Louca, et al., Phys. Rev. B 84 (2011) 054522.
[20] H.H. Chang, et al., Supercond. Sci. Technol. 25 (2012) 035004.
[21] F.-C. Hsu, et al., Proc. Natl. Acad. Sci. 105 (2008) 14262.
[22] J.-F. Ge, et al., Nat. Mater. 14 (2015) 285.
[23] T.M. McQueen, et al., Phys. Rev. B 79 (2009) 014522.
[24] W. Bao, et al., Phys. Rev. Lett. 102 (2009) 247001.
[25] Y.M. Dai, et al., Phys. Rev. B 90 (2014) 121114 (R).
[26] J.C. Zhuang, et al., Appl. Phys. Lett. 104 (2014) 262601.
[27] Y. Sun, et al., Sci. Rep. 6 (2016) 32290.
[28] J. Wen, et al., Phys. Rev. B 86 (2012) 024401.
[29] Z.P. Yin, et al., Nat. Mater. 10 (2011) 932.
[30] T. Hanaguri, et al., Science 328 (2010) 474.
[31] E. Ieki, et al., Phys. Rev. B 89 (2014) 140506 (R).
[32] P.P. Singh, J. Phys.: Condens. Matter 22 (2010) 135501.
[33] S. Chadov, et al., Phys. Rev. B 81 (2010) 104523
J. Kumar, et al., Supercond. Sci. Technol. 25 (2012) 095002
Y. Liu, et al., Phys. Rev. B 92 (2015) 155146.
[34] A. Ceichan et al., Intermetallics 41 (2013) 44.
[35] S. Thirupathaiah, et al., Phys. Rev. B 93 (2016) 205143.
[36] B.C. Sales, et al., Phys. Rev. B 79 (2009) 094521.
[37] C. Liu, et al., Supercond. Sci. Technol. 24 (2011) 035012.
[38] L. Craco, S. Leoni, Mater. Res. Express 1 (2014) 036001.
[39] M. Aichhorn, et al., Phys. Rev. B 82 (2010) 064504.
[40] A. Liebsch, H. Ishida, Phys. Rev. B 82 (2010) 155106.
[41] S.J. Moon, et al., Phys. Rev. Lett. 106 (2011) 217001.
[42] G.F. Chen, et al., Phys. Rev. B 79 (2009) 140509 (R).
[43] G. Kotliar, et al., Rev. Mod. Phys. 78 (2006) 865.
[44] L. Craco, Phys. Rev. B 77 (2008) 125122.
[45] N. Dasari, et al., Eur. Phys. J. B 89 (2016) 202.
[47] K. Haule, G. Kotliar, New J. Phys. 11 (2009) 025021
J. Tomczak, S. Biermann, J. Phys.: Condens. Matter 21 (2009) 064209.
[48] C. Grenzebach, et al., Phys. Rev. B 74 (2006) 195119.
[49] L.-F. Arsenault, A.-M.S. Tremblay, Phys. Rev. B 88 (2013) 205109 see also
A. Romano, J. Ranninger, Phys. Rev. B 62 (2000) 4066.
[50] K. Urasaki, T. Saso, J. Phys. Soc. Jpn. 68 (1999) 3477
T. Saso, J. Phys. Soc. Jpn. 73 (2004) 2894–2899.
[51] L. Baldassarre, et al., Phys. Rev. B 77 (2008) 113107.
[52] M. Hirayama, et al., Phys. Rev. B 87 (2013) 195144.
[53] N. Lanatà, et al., Phys. Rev. B 87 (2013) 045122.
[54] P.L. Bach, et al., Phys. Rev. B 83 (2011) 212506.
[55] E.E. Rodrigues, et al., Phys. Rev. B. 88 (2013) 165110.
[56] All resistivity curves in this work are parametrized in a way to agree with experiment by Chen et al. [42] for the disorder free case, with $n = 6.4$, at 300 K.
[57] A.M. Turner, et al., Phys. Rev. B 80 (2009) 224504.
[58] G. Baskaran, J. Phys. Soc. Jpn. 77 (2008) 113713
S. Pankov, V. Dobrosavljević, Phys. Rev. B 77 (2008) 085104.
[59] O. Gunnarsson, et al., Rev. Mod. Phys. 75 (2003) 1085.
[60] M.S. Laad, et al., Phys. Rev. B 64 (2001) 195114.
[61] L. Craco, et al., Phys. Rev. B 70 (2004) 195116
L. Craco, et al., Phys. Rev. B 73 (2006) 094432.
[62] See, for example, K. Byczuk et al., Phys. Rev. Lett. 90 (2003) 196403.
[63] H. Terletska, et al., Phys. Rev. B 90 (2014) 094208.
[64] See, for example, M.A. Korotin et al., J. Phys.: Condens. Matter 26 (2014) 115501.
[65] G. Garbarino, et al., Phys. Rev. B 84 (2011) 024510.
[66] A. Günther, et al., Supercond. Sci. Technol. 24 (2011) 045009.
[67] I.S. Burmistrov, et al., Phys. Rev. Lett. 108 (2012) 017002.
[68] H. Miao, et al., Nat. Commun. 6 (2015) 6056.